Mine Closure 2026 – AB Fourie, G Boggs, J Heyes & M Tibbett (eds)

doi:10.36487/ACG_repo/2615_49

Three-dimensional dam breach assessment of a closed tailings storage facility using the material point method

Nicolas Pereira [a], **Sudheer S Prabhu** [a,*]

[a] *Geosyntec Consultants, Australia*

Abstract

Dam breach assessments (DBAs) for tailings storage facilities (TSFs) have historically been undertaken using hydraulic modelling approaches developed primarily for operational conditions. However, closure significantly alters key assumptions related to geometry, material behaviour, saturation, and credible failure mechanisms. Recognising these limitations, recent guidance from organisations such as the Canadian Dam Association (CDA) and the US Society on Dams (USSD) encourages the use of advanced numerical models that more realistically represent site-specific conditions, particularly for closed tailings facilities. For mine closure planning, reducing unnecessary conservatism in DBA outcomes is critical to enable risk-informed allocation of closure and post-closure resources.

This paper presents a three-dimensional DBA undertaken for a closed TSF where complex geometry and proximity of critical infrastructure necessitated a fully 3D approach. The assessment was developed directly from a site-specific failure modes and effects analysis (FMEA) updated for closure conditions with all credible failure modes superimposed as a conservative bounding construct rather than a credible compound event. Initial DBAs for the site, based on conventional hydraulic modelling with rheological assumptions, predicted extensive inundation of nearby office infrastructure. These outcomes were reassessed using a material point method (MPM) model, which explicitly incorporates geotechnical material behaviour and large-deformation failure mechanics.

The 3D MPM results demonstrated that, under worst-case breach scenarios, inundation of the relevant infrastructure was not predicted when mean material properties were adopted. To further strengthen confidence in the findings, a statistical sensitivity analysis was undertaken by varying key dam parameters by one and two standard deviations. The results showed that even under these reduced-strength cases, predicted inundation remained limited in extent. The study highlights the value of three-dimensional, physically based modelling for DBAs at closed TSFs, demonstrating how advanced numerical methods can refine consequence estimates and support more defensible, risk-informed mine closure decision-making.

Keywords: *material point method, dam breach assessment, DBA, MPM*

1 Introduction

Dam breach assessments (DBAs) are a fundamental component of consequence classification and emergency response planning for tailings storage facilities (TSFs). Historically, DBAs have been undertaken using hydraulic modelling tools that treat tailings as fluids governed by rheological properties such as yield stress and viscosity, together with pre-defined embankment breach geometries derived from empirical relationships developed for water retaining dams (Froehlich 2016; Zhang et al. 2013). However, guidance developed for water dams does not adequately address the geotechnical considerations specific to tailings outflows (CDA 2021).

* Corresponding author.

For closed facilities, key assumptions inherent in conventional hydraulic DBA approaches are no longer valid. Closure typically involves removal of the supernatant pond, installation of low-permeability capping systems, development of unsaturated crust layers, and progressive decline of phreatic levels within the tailings mass. Under these conditions, tailings behaviour is governed predominantly by soil mechanics rather than fluid rheology. These conditions align with CDA Case 2A or 2B (liquefiable or non-liquefiable tailings without a supernatant pond), for which the CDA (2021) recognises use of numerical models based on continuum mechanics.

Application of hydraulic models to closed TSFs can therefore introduce conservatism and non-credible failure mechanisms, particularly where embankments have been re-profiled and stabilised as part of closure works. In addition, the assumption of a predefined breach geometry does not account for the resistance provided by the embankment during failure. For mine closure planning, overly conservative DBA outcomes can drive disproportionate mitigation measures, such as infrastructure relocation or exclusion zones, that may not be commensurate with actual risk.

The material point method (MPM) has recently gained acceptance for modelling large-deformation problems in geotechnical engineering, including tailings dam breach analyses (Zabala & Alonso 2011; Robertson et al. 2019; Pierce 2021). Ramírez et al. (2025) noted that MPM is well suited for certain dam break scenarios (Case 2A and 2B scenarios in CDA, 2021), as it treats tailings as a soil governed by shear strength and can therefore simulate both failure initiation and post-failure runout within a single framework.

This paper presents a three-dimensional (3D) MPM-based DBA undertaken for a closed TSF where complex embankment geometry and proximity of site infrastructure required a fully 3D assessment. The objectives of the study were to reassess previously predicted inundation outcomes under current closure conditions and to evaluate the credibility of the outcomes through a structured sensitivity analysis. In addition, this paper presents an approach for deriving inundation maps directly from MPM simulation outputs, a key deliverable for consequence classification and emergency planning that has not previously been demonstrated using MPM.

2 Site description and facility configuration

2.1 Facility overview

The closed facility considered in this study is located in Australia and was operated as a downstream-raised embankment for tailings storage. Following cessation of operations, the facility was closed and re-profiled into a shedding landform incorporating perimeter drains and surface water management features. A low-permeability capping system comprised of a geomembrane, cover soils and vegetation was installed to limit rainwater infiltration.

As a result of the closure works, the facility has no surface water storage capacity. Piezometric monitoring indicated sustained decline in phreatic levels since deposition ceased and decant pond removal. Groundwater modelling indicated that phreatic levels will continue to decline over time. Consequently, flood-day failure scenarios were non-credible. Therefore this assessment only considered sunny-day failure scenarios. As it is noted in the subsequent sections, based on the cone penetration tests (CPTs), some of the tailings were saturated and liquefiable. This scenario is consistent with CDA Case 2A.

2.2 Embankment geometry

The embankment geometry is complex and non-uniform due to the facility’s construction history. The original embankment was constructed with uniform upstream and downstream slopes of approximately 1V:3H (western embankment). Subsequent facility extensions modified the downstream geometry, resulting in spatially varying slopes. In the eastern portion of the facility, the upstream and downstream embankment slopes are approximately 1V:2H and 1V:4H, respectively. The tailings closure surface throughout the facility has an overall slope of approximately 1V:10H. The embankment height is approximately 12 m and the crest width is approximately 10 m.

The full post-closure geometry, including embankment slopes, tailings surface, site infrastructure and perimeter drains, is shown in Figure 1. This spatial variability in embankment geometry was explicitly incorporated into the 3D numerical model.

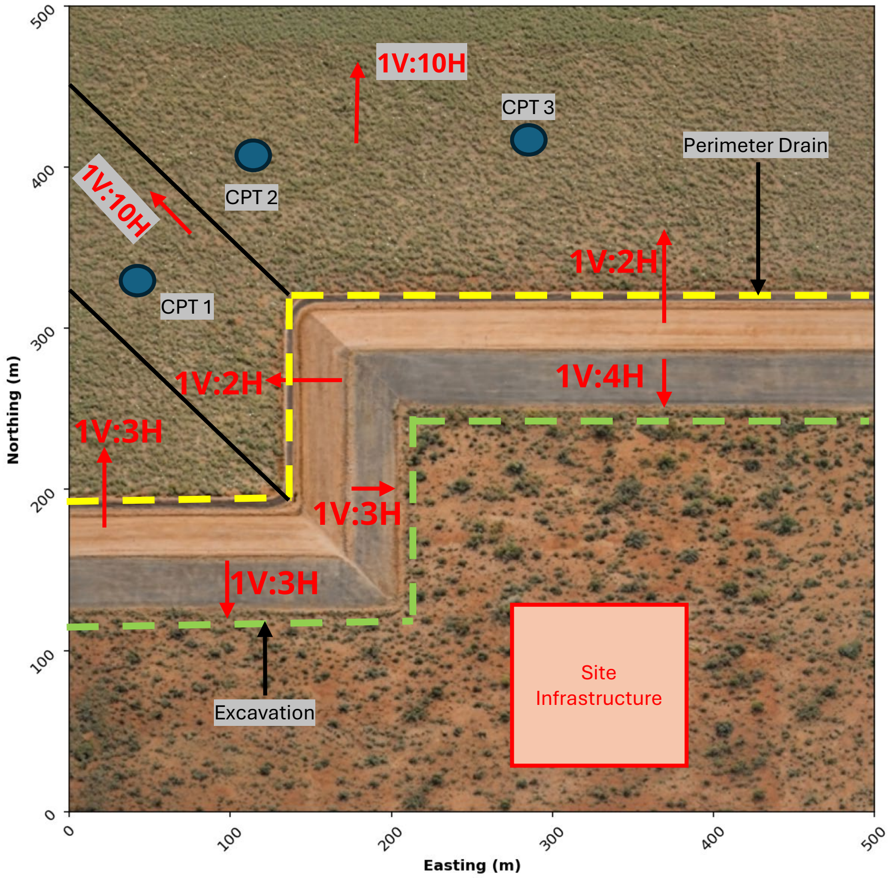

Figure 1 Plan view of the TSF showing embankment geometry, slope configurations (1V:2H, 1V:3H, and 1V:4H), tailings closure surface slope (1V:10H), location of site infrastructure, and perimeter drains

2.3 Site infrastructure

Site infrastructure is located downstream of the embankment. The proximity of this occupied infrastructure was a primary driver for undertaking a 3D assessment. Previous DBAs conducted during the operational phase predicted extensive inundation of the surrounding area, raising concerns for closure planning.

2.4 Failure modes assessment

Failure scenarios were developed based on a site-specific failure modes and effects analysis (FMEA). Three sunny-day failure mechanisms were identified as credible based on the FMEA:

1. Excavation at the embankment toe, resulting in loss of passive resistance and potential slope instability.
2. Foundation collapse, involving post-peak strength loss in a weak alluvial foundation layer beneath the embankment.
3. Seismic-induced failure, involving liquefaction of saturated contractive tailings and reduction in embankment strength.

The three mechanisms were applied simultaneously as a bounding construct, not as a credible real-world event, to define an upper-bound loss of resistance for consequence assessment.

3 Methodology

3.1 Numerical method

The MPM is a hybrid Eulerian–Lagrangian numerical technique in which material points carry material properties and state variables through a fixed background grid. At each time step, governing equations are solved on the grid and mapped back to the material points, allowing simulation of large deformations without mesh distortion (Sulsky et al. 1994).

The analyses were performed using MPoint (Purvence and Coetzee, 2024; Pereira et al, 2025), developed by Itasca Consulting Group. The model represented embankment materials, foundation soils, tailings crust and contractive tailings as distinct material domains.

3.2 3D model setup

The model domain consisted of the embankment, tailings and the downstream area including the site infrastructure footprint. The site infrastructure itself was not explicitly modelled, as the objective was to assess tailings inundation extent and depth rather than structural response.

The post-closure geometry was derived from the recent survey data. A regular background grid with 2 m spacing was used, with two material points per cell, resulting in a minimum material point size of approximately 1 m. Figures 2 to 5 illustrate the plan view and cross-sections in the model. Cover soils and geomembranes accounted for 0.5 m on top of the tailings crust and were not considered in the model.

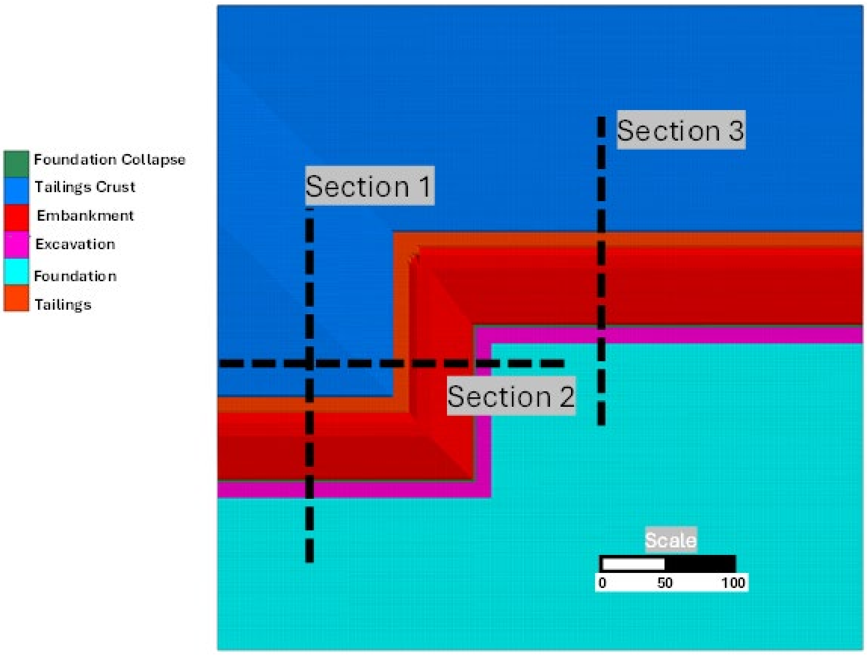

Figure 2 Plan view of the 3D model showing the spatial distribution of material zones

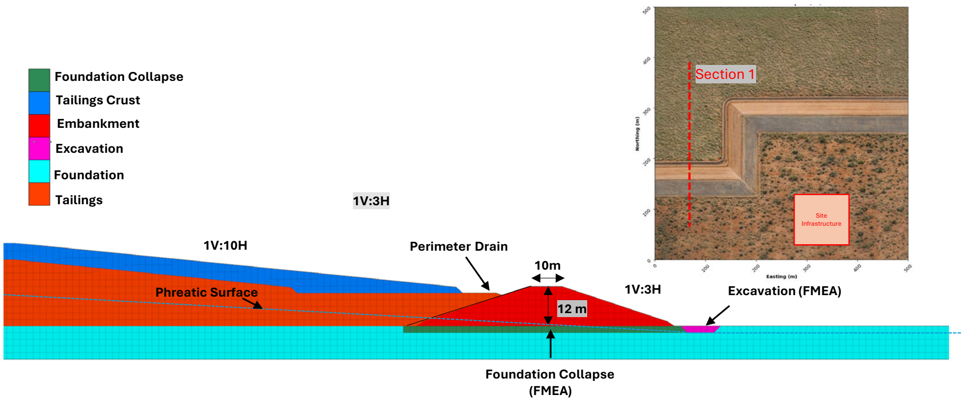

Figure 3 Cross-section 1 shown in the model

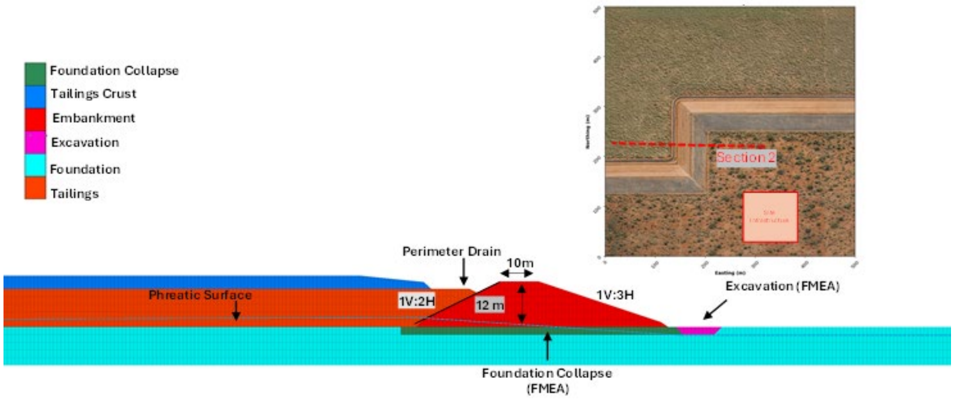

Figure 4 Cross-section 2 shown in the model

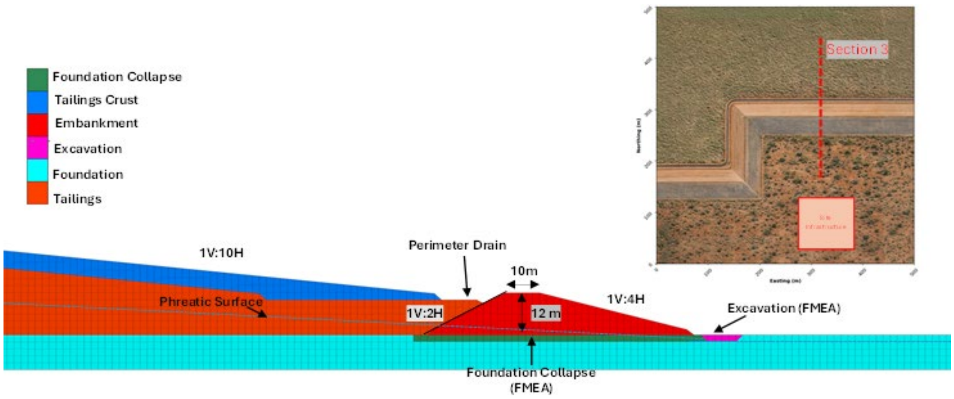

Figure 5 Cross-section 3 shown in the model

The identified failure modes from the FMEA were introduced in the model though different methodologies. The excavation was adopted in the model by removing the elements (12 m wide and 2 m deep) throughout the toe of the embankment (see Figures 1–5). The foundation collapse was simulated by applying residual shear strength properties 2m of foundation soil below the entire embankment extent (see Figures 3–5).

3.3 Statistical sensitivity approach

To quantify the influence of material strength variability on breach outcomes, a statistical sensitivity analysis was undertaken. Three cases were analysed:

- Case 1: mean (μ) material properties

- Case 2: mean minus one standard deviation (μ − σ), equivalent to the 15.9th percentile
- Case 3: mean minus two standard deviations (μ − 2σ), equivalent to the 2.3rd percentile.

A coefficient of variation of 25 % was adopted to estimate standard deviation, consistent with Phoon (2008). This approach provides a structured assessment of robustness without the computational burden of full probabilistic analysis.

3.4 Inundation map development

Inundation maps were developed directly from the MPM simulation outputs by comparing pre- and post-simulation elevations at each grid location. Areas where the final elevation exceeded the initial elevation were classified as positively inundated, with the difference representing the inundation depth. Locations where the initial elevation exceeded the final elevation (negative inundation) indicate settlement or lateral displacement of material during the simulated breach. This approach enabled the generation of spatial inundation maps that are directly comparable to those produced by conventional hydraulic models.

4 Material properties

A detailed discussion of the material property interpretation and characterisation is outside the scope of this paper; however, a brief overview is provided in this section. The adopted properties were noted to be consistent with published ranges for similar materials in literature and the properties are summarised in Table 1. Young's modulus and Poisson's ratio are small-strain elastic properties. Given that tailings runout is fundamentally a large-strain problem, these parameters have minimal influence on the results. Therefore, a Young modulus of 100,000 kPa and a Poisons ratio of 0.33 were used for all the materials in the simulations.

Table 1 Material properties used in the simulation

Geotechnical unit	Unit weight (ton/m^3)	Cohesion (kPa)	Friction	s_u/σ'_v (peak)	s_r/σ'_v (residual)
Foundation (collapse)	19	NA	NA	NA	0.15 Min. 25 kPa
Foundation (general)	19	0	27	NA	NA
Embankment (above phreatic)	21	0	Case 1: 30.0 Case 2: 23.4 Case 3: 16.1	NA	NA
Embankment (below phreatic)	18	NA	NAff	Case 1: 0.28; Min. 50 kPa Case 2: 0.21 Min. 37.5 kPa Case 3: 0.14; Min. 25 kPa	NA
Tailings (crust)	16	NA	Case 1: 30.0 Case 2: 23.4 Case 3: 16.1	NA	NA
Tailings	16	NA	NA	NA	0.01; Min. 2 kPa

4.1 Embankment

The embankment at the site was constructed using compacted silty sand fill material. Although the embankments were compacted, the embankment materials were conservatively assumed to exhibit undrained behaviour below the phreatic surface and drained above the phreatic surface. The drained and undrained properties noted in Table 1 were derived based on the triaxial testing of the material at relevant stress levels.

For the embankment material above the phreatic surface, a mean friction angle (μ) of 30° was adopted. For the portion below the phreatic surface, an undrained shear strength ratio (s_u/σ'_v) of 0.28 with a minimum strength of 50 kPa was used for Case 1, with strength reducing for Cases 2 and 3 as detailed in Table 1.

4.2 Foundation

The foundation comprises medium stiff to stiff alluvium underlain by a very stiff to hard residual stratum. Drained shear strength for the foundation was characterised by a friction angle of 27°, interpreted from standard penetration test data. To simulate foundation collapse, the upper 2 m of the alluvial layer was assigned a post-peak undrained shear strength ratio (sr/σ'v) of 0.15 with a minimum shear strength of 25 kPa.

4.3 Tailings

CPTs at the site (shown in Figure 1) were interpreted using the methods proposed by Lunne et al. (1997) and Robertson (2010) for residual shear strength ratio (s_r/σ'_v) and Plewes et al. (1992) for state parameter (ψ). The interpreted results from the CPTs are shown in Figure 6.

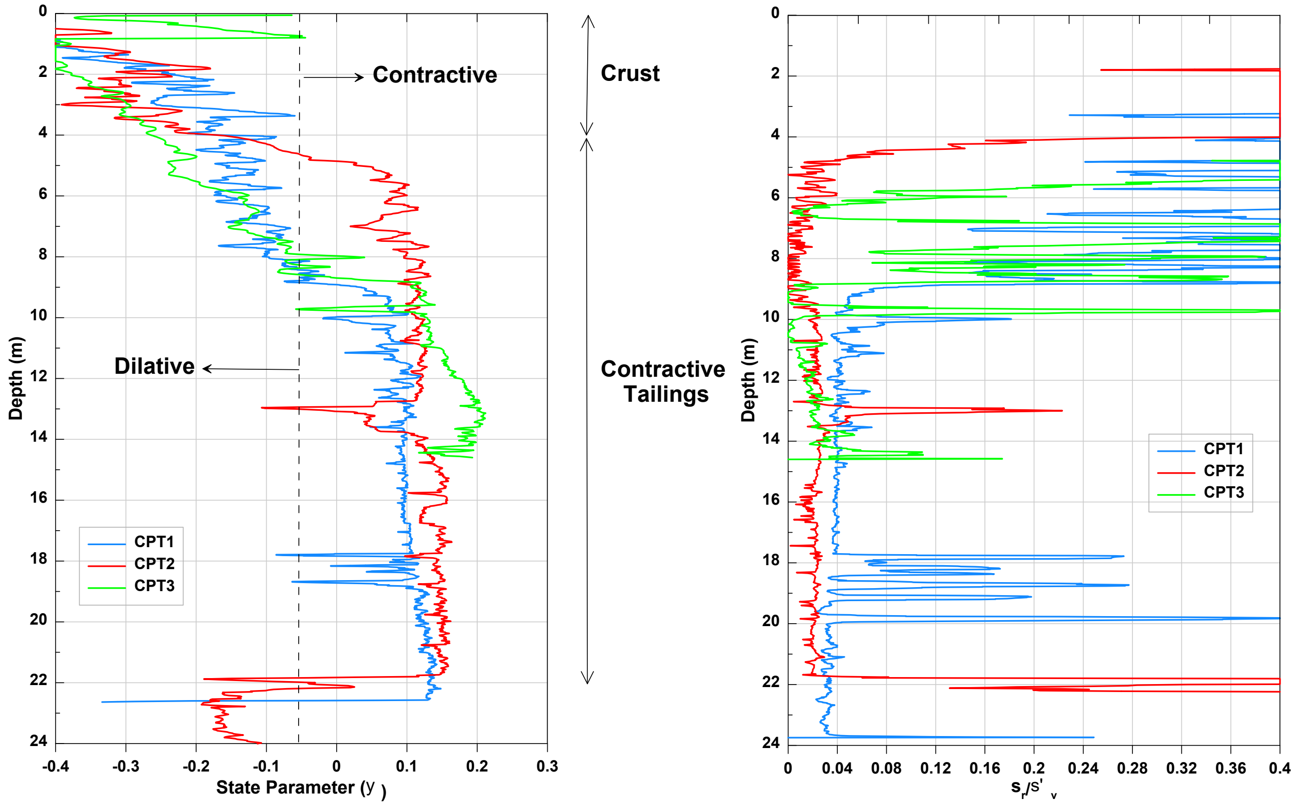

Figure 6 CPT interpretation results for CPTs 1, 2, and 3 showing state parameter (ψ) and residual undrained strength ratio (s_r/σ'_v) with depth

Based on Figure 6, tailings were characterised as tailings crust and contractive tailings as follows.

- Tailings crust: the upper tailings were characterised by dilative state parameters (ψ < −0.05) (refer to Figure 6) although high u2 (>200 kPa) values were noted in this layer indicating saturated or near saturated conditions. Due to these characteristics, the crust was considered non-liquefiable with a friction angle of 30° for Case 1, with reductions for Cases 2 and 3. The lowest crust thickness of 4 m was noted at CPT 2 while at the other locations, the crust thickness was higher. Therefore, throughout the model, a uniform crust thickness of 4 m was adopted (shown in Figures 3–5).

- Contractive tailings: as shown in the CPT plot in Figure 2, below the crust, the CPTs indicate tailings to be contractive and liquefiable. The lowest 20th percentile residual strength ratio (sr/σ'v) value ranged from 0.01 to 0.03 among the CPTs. The lowest value of 0.01, with a minimum of 2 kPa, was conservatively adopted for all cases though out the contractive tailings.

4.4 Phreatic Surface

The phreatic surface adopted in the 3D model was based on the vibrating wire piezometers (VWPs) within the model domain. A 3D phreatic surface was developed based on VWPs by interpolation and implemented in the model. Figures 3–5 shows the phreatic surface at different cross sections.

5 Results

Three material strength cases were simulated, representing progressively more conservative strength assumptions. In all cases, tailings release was predicted, with the capping geomembrane breached and the perimeter drains inundated, rendering them non-functional. Results for each case are discussed in the following sections.

5.1 Case 1: mean properties (μ)

Results from the model are shown in Figures 7–9. Under mean material properties, the model predicted tailings release from the facility, with material progressing downstream from the embankment toe. However, the extent of travel was limited, and inundation did not approach the site infrastructure. Figure 7 shows the predicted deposition in plan view, while Figure 8 shows the same results with respect to Sections 1, 2 and 3.

Upstream of the embankment, significant deformation was predicted due to residual strength being applied to the contractive tailings underlying the crust, resulting in flattening of the 1V:10H closure slope. This deformation would be expected to cause geomembrane distress where the capping layer overlies the tailings crust. The perimeter drain was inundated throughout the facility, rendering it non-functional. On the downstream side, the greatest inundation extent was predicted from the eastern embankment section (Section 3), which had the mildest downstream slope of 1V:4H.

Figure 9 shows the inundation map for Case 1, with colours representing locations where the post-simulation surface elevation exceeded the pre-simulation elevation. Inundation depths peak near the embankment crest and decrease progressively downstream, with the inundation extent stopping well short of the site infrastructure.

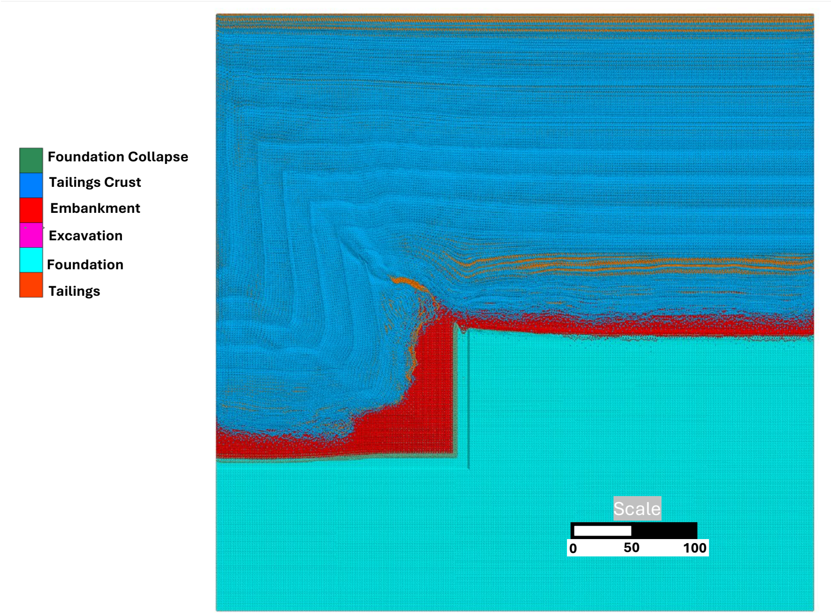

Figure 7 Case 1 (μ): plan view of material distribution at the end of simulation showing embankment deformation and tailings runout relative to the site infrastructure

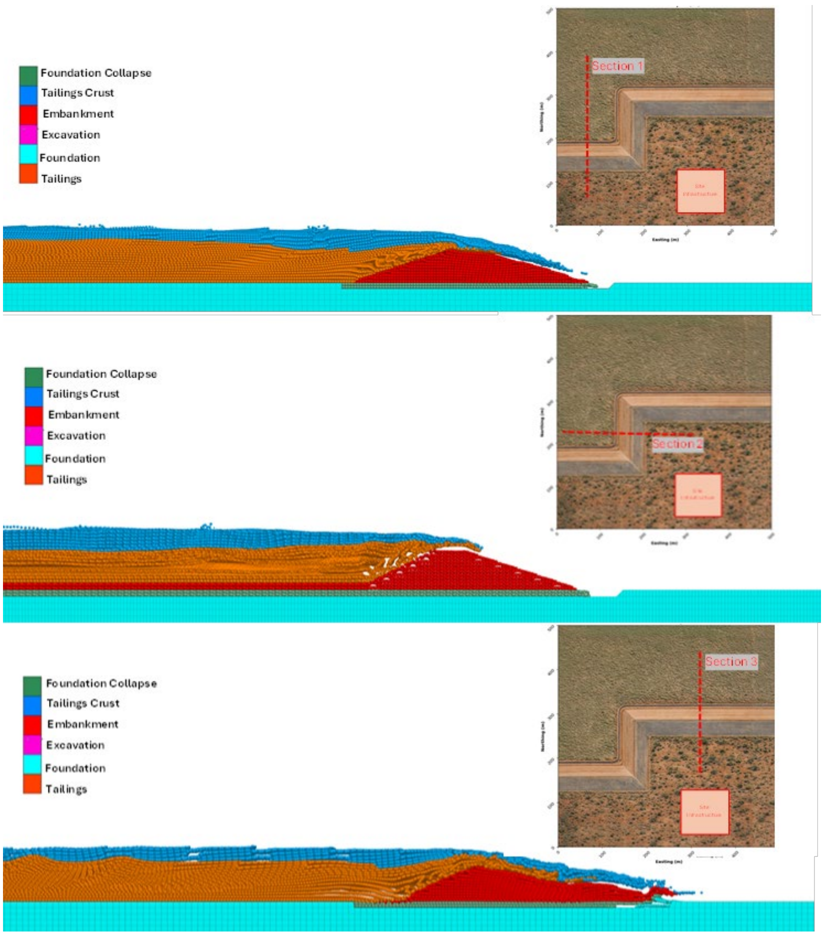

Figure 8 Case 1 (μ): cross-sectional results for Sections 1, 2 and 3

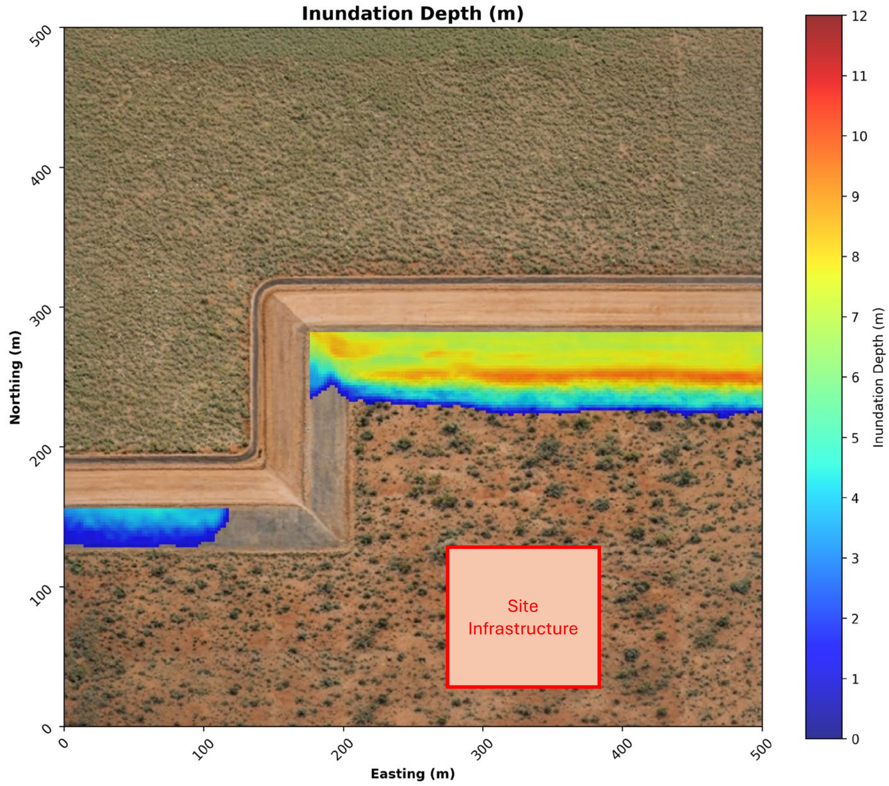

Figure 9 Case 1 (μ): inundation map showing spatial distribution of positive inundation depth

5.2 Case 2: mean minus one standard deviation (μ − σ)

Results from the model are shown in Figures 10 through 12. In Case 2 (μ − σ, 15.9th percentile shear strength for crust and embankment), the model predicted increased runout relative to Case 1. The extent of tailings release was greater, and embankment deformation was more pronounced due to the reduced shear strength of the embankment and tailings crust. However, the modelled inundation did not reach the site infrastructure. Figure 10 shows the material distribution in plan view, and Figure 11 presents the cross-sectional results for Sections 1, 2 and 3.

Upstream of the embankment, geomembrane distress was predicted to be more extensive than in Case 1, with greater deformation observed across the tailings surface adjacent to the embankment crest. On the downstream side, the flatter 1V:4H section in the middle of the downstream face, a consequence of the facility extension, provided greater runout length than the western embankment, which had a steeper 1V:3H downstream slope.

Figure 12 presents the inundation map for Case 2. The inundation footprint is larger than Case 1, with greater depths predicted immediately downstream of the embankment crest. Areas upstream of the embankment without inundation reflect lateral displacement of tailings, consistent with the deformation behaviour described above. The inundation extent does not reach the site infrastructure.

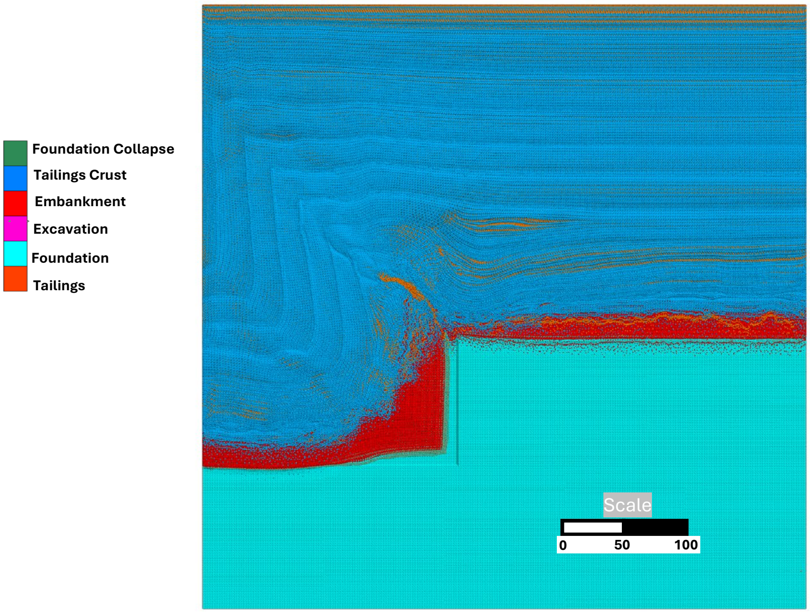

Figure 10 Case 2 (μ − σ): plan view of material distribution at the end of simulation

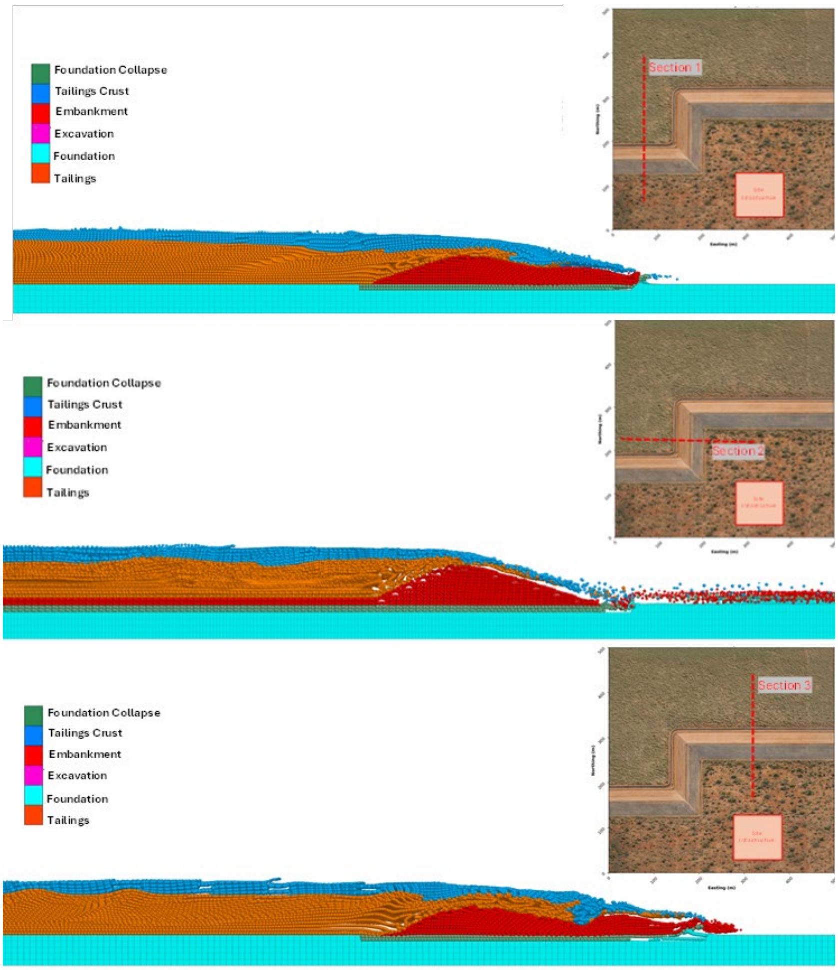

Figure 11 Case 2 (μ − σ): cross-sectional results for Sections 1, 2 and 3

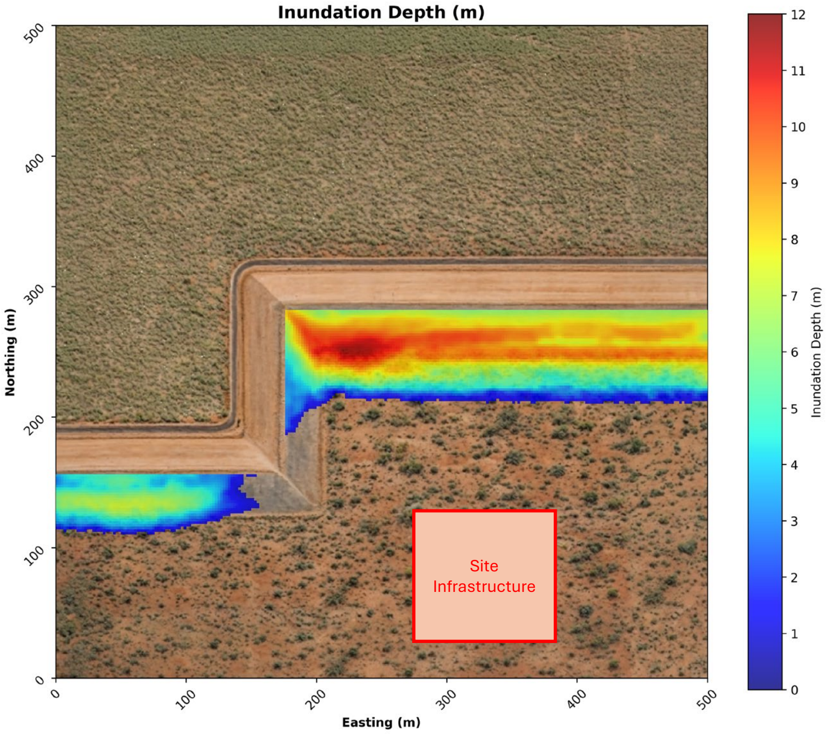

Figure 12 Case 2 (μ − σ): inundation map showing spatial distribution of positive inundation depth

5.3 Case 3 — Mean Minus Two Standard Deviations (μ − 2σ)

Results for Case 3 are shown in Figures 13–15. Representing the most conservative scenario, with shear strengths at the 2.3 percentile of the plausible range, this case produced the largest runout extent of all three cases, with mobilised material extending further downstream than in Cases 1 and 2. Figure 13 shows the material distribution in plan view and Figure 14 presents cross-sectional results for Sections 1, 2 and 3.On the upstream side, large settlements were predicted across the tailings surface.

On the downstream side, the greatest inundation extent was predicted from the eastern embankment where the mildest slope of 1V:4H is present, consistent with Case 1. Material displacement from the western embankment (Section 1) was also greater than in previous cases. Despite this, the overall travel distance remained limited.

Figure 15 presents the inundation map for Case 3. Inundation depths are highest in this case at both the eastern and western embankment as well. Although the runout is noted to be higher compared to the previous Cases, it is limited and does not reach the site infrastructure area.

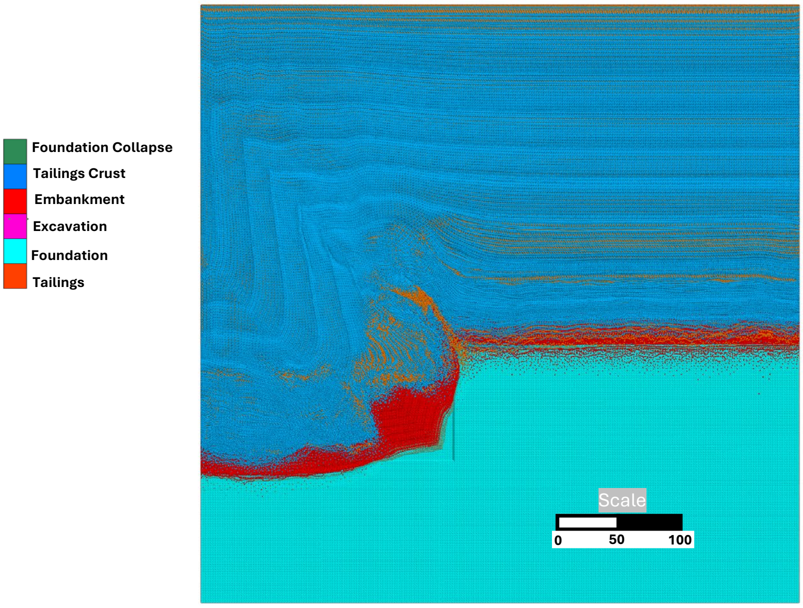

Figure 13 Case 3 (μ – 2σ) — Plan view of material distribution at the end of simulation

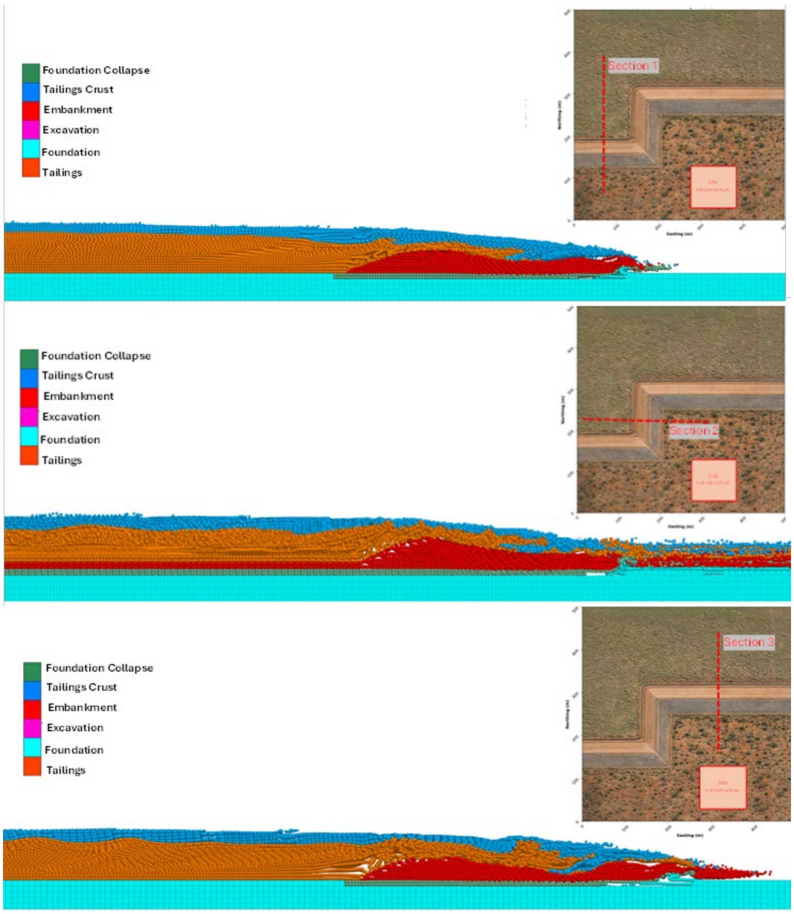

Figure 14 Case 3 (μ – 2σ): cross-sectional results for Sections 1, 2 and 3

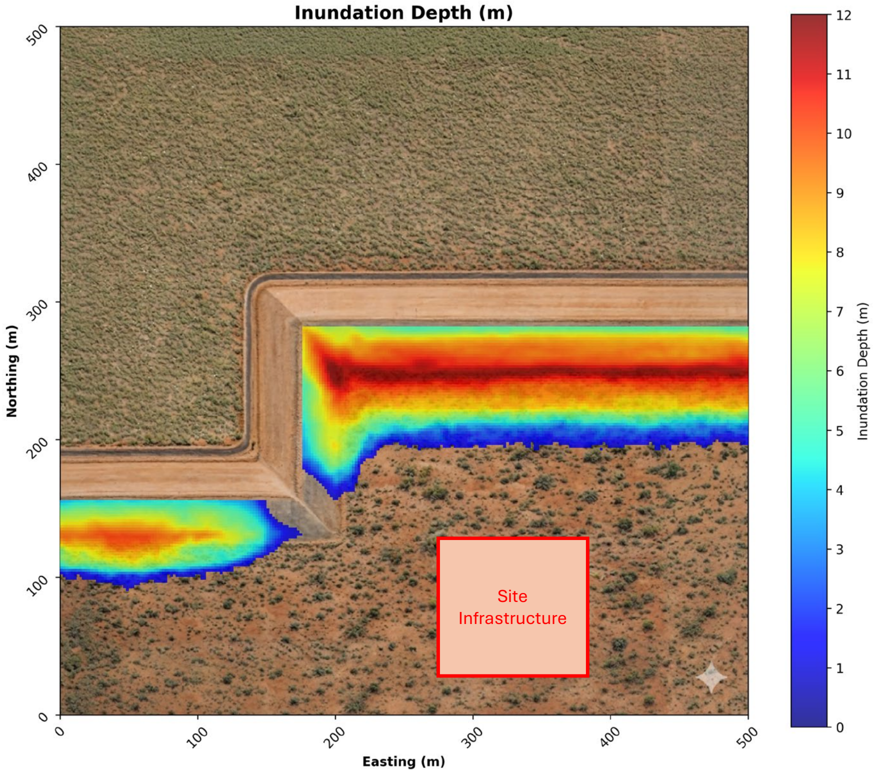

Figure 15 Case 3 (μ – 2)L inundation maps showing spatial distribution of positive inundation depth

6 Discussions

6.1 Comparison with previous DBA outcomes

The initial DBAs for this facility, conducted during the operational phase using conventional hydraulic models with rheological assumptions, predicted extensive inundation of the site infrastructure downstream of the embankment. Those predictions were based on conditions no longer representative of the facility due to (i) the presence of a supernatant pond (ii) high phreatic levels and (iii) tailings assumed to behave as a viscous fluid. The 3D MPM assessment demonstrates that, under the current closed and capped conditions, both the runout extent and inundation are significantly reduced, with the site infrastructure remaining clear across all cases analysed.

6.2 Implications for mine closure

The progressive increase in runout extent from Case 1 through Case 3 demonstrates that the model responds consistently to strength reduction, as expected. Even under the most conservative strength assumptions (Case 3, $\mu - 2\sigma$) and all failure modes assumed to act simultaneously, no inundation was noted in the vicinity of the site infrastructure. This provides a high level of confidence that the site infrastructure will not be impacted in the event of a dam breach.

The previous hydraulic model predictions necessitated costly mitigation measures, such as relocation of infrastructure, construction of engineered barriers, or imposition of exclusion zones. The refined 3D MPM results demonstrate that these measures may not be warranted under the current closed conditions.

More broadly, the outcomes of this study are directly relevant to relinquishment and legacy management planning. A physics-based 3D DBA provides a more representative basis for characterising residual risk at a closed facility, which in turn supports the setting of closure objectives and criteria, the design of the final landform and surface water management features, and the long-term monitoring and maintenance commitments that must be demonstrably manageable for relinquishment to be credible.

6.3 Geomembrane distress and perimeter drain functionality

Across all cases, the model predicted significant deformation of the tailings crust upstream of the embankment due to the imposed residual strengths on the underlying contractive tailings below the 1V:10H slope adopted at the site for closure. As the capping geomembrane is placed directly on the crust surface, it is reasonable to assume that deformations of the crust would translate to comparable strains in the geomembrane. The magnitude of the predicted deformations suggests that the geomembrane would experience significant distress and is unlikely to remain functional following any breach event.

In addition, the perimeter drains located immediately upstream of the embankment are noted to be flattened due to the breach event and are expected to be inundated by mobilised tailings in all cases, rendering them non-functional. While neither the geomembrane distress nor the loss of perimeter drain functionality directly affects the downstream inundation outcome, these are useful secondary outputs of the 3D MPM model that provide additional insight into post-breach facility conditions. Such outputs can inform closure maintenance planning, long-term monitoring requirements, and post-event remediation strategies.

7 Conclusions

A three-dimensional dam breach assessment was undertaken for a closed TSF using the MPM, consistent with CDA Case 2A (liquefiable tailings without a supernatant pond). Three credible sunny-day failure modes were identified from a site-specific FMEA and applied concurrently: (1) excavation at the embankment toe, (2) foundation collapse, and (3) tailings liquefaction and embankment strength reduction due to earthquake. Three material strength cases were analysed: Case 1 (mean, μ), Case 2 ($\mu - \sigma$), and Case 3 ($\mu - 2\sigma$). The key findings are:

- Under mean material properties (Case 1), tailings release was predicted; however, the runout extent was limited. Inundation of the site infrastructure was not expected.
- Under $\mu - \sigma$ (Case 2), the runout extent increased relative to Case 1. The site infrastructure remained outside the expected inundation zone.
- Under $\mu - 2\sigma$ (Case 3), the largest runout extent was noted. However, runout does not reach the site infrastructure.

Capping geomembrane distress is expected upstream of the embankment across all cases due to tailings liquefaction and associated slope flattening. The perimeter drain is expected to be inundated and rendered non-functional in all cases.

Previous DBAs using conventional hydraulic models predicted extensive site infrastructure inundation. The 3D MPM results demonstrate these predictions are not representative of the current closed conditions.

The study highlights the value of three-dimensional, geotechnical-based modelling for DBAs at closed TSFs, demonstrating how advanced numerical methods can refine consequence estimates and support more defensible, risk-informed mine closure decision-making.

References

Froehlich, DC 2016, 'Embankment dam breach parameters and their uncertainties', *Journal of Hydraulic Engineering*, vol. 142, no. 12.

Sulsky, D, Chen, Z & Schreyer, HL 1994, 'A particle method for history-dependent materials', *Computer Methods in Applied Mechanics and Engineering*, vol. 118, pp. 179–196.

Plewes, HD, Davies, MP & Jefferies, MG 1992, CPT based screening procedure for evaluating liquefaction susceptibility, *Proceedings of the 45th Canadian Geotechnical Conference*, Toronto, pp. 41–49.

Ramírez, EL, Ledesma, O & Lizcano, A 2025, 'Runout analysis using the material point method (MPM) for CDA cases 2A and 2B', *Proceedings of the Canadian Dam Association (CDA) Annual Conference 2025*.

Canadian Dam Association (CDA) 2021, *Technical Bulletin: Tailings Dam Breach Analysis*, Toronto.

Lunne, T, Robertson, PK & Powell, JJM 1997, *Cone Penetration Testing in Geotechnical Practice*, Spon Press, London.

Phoon, KK 2008, Reliability-based design in geotechnical engineering: Computations and applications, Taylor & Francis.

Pierce, I 2021, *Applying the Material Point Method to Identify Key Factors Controlling Runout of the Cadia Tailings Dam Failure of 2018*, MSc thesis, Virginia Tech, Blacksburg.

Purvance, M & Coetzee, C 2024, MPAC – Material Point Analysis of Continua, Hazzard, Katsaga, Sanftenberg & Nelson (eds), *Applied Numerical Modeling in Geomechanics – 2024, Itasca International Inc.*, Minneapolis, Paper 13-01, ISBN 978-0-9767577-6-4.

Robertson, PK 2010, Cone Penetration Testing in Geotechnical Engineering: Practice and Applications, Elsevier, Amsterdam.

Robertson, PK, de Melo, L, Williams, DJ & Wilson, GW 2019, *Report of the Expert Panel on the Technical Causes of the Failure of Feijão Dam I*, Expert Panel Report commissioned by Vale.

Zabala, F & Alonso, EE 2011, 'Progressive failure of Aznalcóllar dam using the material point method', *Géotechnique*, vol. 61, no. 9, pp. 795–808.

Zhang, LM, Xu, Y & Zhang, S 2013, 'Breaching parameters for earth and rockfill dams', *Journal of Geotechnical and Geoenvironmental Engineering*, vol. 139, no. 12, pp. 1987–2001

Pereira, N, Prabhu, SS, Purvance, M, Coetzee, C & Loffell, D 2025, 'Dam breach analysis of a closed facility using the Material Point Method', in S Knutsson, AB Fourie & M Tibbett (eds), *Mine Closure 2025: Proceedings of the 18th International Conference on Mine Closure*, Australian Centre for Geomechanics, Perth, https://doi.org/10.36487/ACG_repo/2515_45